Journal of *Marine Science and Engineering*

MDPI

Article

Assessing the Changes in Precipitation Patterns and Aridity in the Danube Delta (Romania)

Alina Bărbulescu [1] and Cristian Ștefan Dumitriu [2,*]

[1] Department of Civil Engineering, Transilvania University of Brașov, 5 Turnului Str., 500152 Brașov, Romania; alina.barbulescu@unitbv.ro
[2] Faculty of Mechanical Equipment for Constructions and Robotics, Technical University of Civil Engineering, 59 Calea Plevnei, 021242 Bucharest, Romania
* Correspondence: cristian.dumitriu@utcb.ro

Abstract

Understanding long-term precipitation variability is essential for assessing the climate's impact on sensitive ecosystems, particularly in regions of high environmental value, such as the Danube Delta Biosphere Reserve (DDBR). This study examines the temporal dynamics of monthly precipitation in the Danube Delta, Romania, spanning the period from 1965 to 2019. Three approaches were used to analyze climatic variability: Change Point detection (CPD) to identify shifts in precipitation regimes, the De Martonne Index (I_M) to assess aridity trends, and the Standardized Precipitation Index (SPI) to evaluate drought conditions across annual and monthly scales. Using robust monthly precipitation and temperature datasets from the Sulina meteorological station, CPD analysis revealed statistically significant structural breaks in precipitation trends, suggesting periods of altered climate behavior likely associated with broader regional or global climate changes. I_M values indicated mostly hyper-aridity and aridity at monthly and annual scales, respectively. No monotonic trend was found in this index during the analyzed segments, as emphasized by the Mann–Kendall (MK) test. SPI values provided further evidence of variability in the precipitation regime, highlighting a transition toward more extreme hydrological conditions in the region. The combined use of these indices offers a comprehensive view of the evolution of climatic conditions in the Danube Delta. The findings underscore the growing vulnerability of this unique wetland ecosystem to climatic variability, supporting the need for adaptive water management strategies in the face of anticipated future changes.

Keywords: CPD; cumulative sum (CUSUM); I_M; SPI; trend

Academic Editors: Jinyu Sheng, Georg Umgiesser, Harold Ritchie, Youyu Lu, Natacha B. Bernier and Michael Dowd

Received: 12 June 2025
Revised: 23 July 2025
Accepted: 7 August 2025
Published: 9 August 2025

Citation: Bărbulescu, A.; Dumitriu, C.Ș. Assessing the Changes in Precipitation Patterns and Aridity in the Danube Delta (Romania). *J. Mar. Sci. Eng.* **2025**, *13*, 1529. https://doi.org/10.3390/jmse13081529

1. Introduction

Climate change has become a major environmental concern in recent decades, with significant consequences for water resources. Understanding these modifications, the mechanism, and coverage is essential for the sustainable management of water systems, safeguarding public access to water, and reducing the negative influence of human activities on water quality.

Precipitation is a fundamental component of water cycles in nature, governing water availability, supporting ecosystems, and sustaining human livelihoods [1]. In recent decades, both observational data and climate model projections have indicated that rainfall intensity, frequency, and distribution have undergone significant changes under the influence of ongoing climate modifications [2]. As temperatures rise at the planetary level,

atmospheric movement and humidity are being altered, disrupting the known precipitation patterns [3]. A notable consequence of atmospheric temperature augmentation is the enhanced availability of humidity retention (approximately 7% per 1 °C), which leads to an increase in the intensity of extreme events [4]. At the same time, shifts in large-scale atmospheric circulation patterns are modifying the geographic distribution, type, and seasonality of precipitation [5]. Consequently, certain areas are experiencing the amplification and intensification of flood events, while others are undergoing reduced precipitation and prolonged dry spells. These shifts have far-reaching implications for freshwater resources, the resilience of ecosystems, agricultural sustainability, and disaster preparedness [6–9]. Climate projections suggest that these trends will persist if significant measures to reduce greenhouse gas emissions (the primary driver of these changes) are not implemented [10–12].

Over the past six decades, the South East Europe (SEE) region, comprising countries such as Albania, Bulgaria, Greece, Romania, Serbia, North Macedonia, and parts of Turkey, has undergone significant climatic transformations influenced by both global and regional factors. Situated at the confluence of the Mediterranean, continental, and mountainous climatic zones, this region is particularly vulnerable to climate change. The period following 1960 has notably marked the commencement of an accelerated warming trend, with discernible implications for natural ecosystems, socio-economic sectors, and regional climate systems. Recorded data and regional climate assessments reveal a considerable increase in mean annual temperatures across SEE, with most sub-regions experiencing a warming rate exceeding 1.0 °C since 1960 [13–15]. This warming trend has intensified since the 1980s, particularly during the summer months, resulting in more frequent and prolonged heatwaves, reduced soil moisture, and increased thermal stress in both urban and rural contexts [16–18]. Concurrently, precipitation patterns have exhibited significant spatial and seasonal variations. Southern and coastal sub-regions, including parts of Greece and Albania, are characterized by declining summer precipitation and an increase in the frequency of drought occurrences.

By contrast, certain northern and mountainous areas have experienced modest increases in winter precipitation, often accompanied by a decrease in snowfall and an earlier onset of snowmelt. These developments are affecting the hydrological regimes of major river systems, such as the Danube, Vardar, and Maritsa, thereby exerting downstream impacts on agriculture, energy production, and ecosystem services. The escalation of extreme weather events, including flash floods, convective storms, and wildfires, further highlights the region's growing vulnerability to climate change. Factors such as urbanization, land use modifications, and inadequate adaptive infrastructure exacerbate these risks, particularly in densely populated and economically vulnerable areas [19–22].

Looking ahead, regional climate projections indicate that SEE is expected to continue warming at a rate that surpasses the global average under high-emission scenarios, with an anticipated mean temperature increase of 2–4 °C by mid-century. Additionally, precipitation extremes, seasonal water shortages, and shifts in biodiversity are projected to intensify unless substantial efforts are undertaken to mitigate and adapt to climate impacts. Within this framework, understanding the evolution of climate trends in the SEE region since 1960 is crucial for informing national policies, promoting regional collaboration, and developing sustainable planning initiatives [13,23].

Agriculture in SEE is particularly vulnerable to climatic variability due to its reliance on rain-fed systems, fragmented landholdings, and limited adaptive capacity among smallholder farmers. The sector not only plays a vital economic role in many countries of the region but also maintains socio-cultural and environmental functions that are integral to rural communities. Crop yields, planting seasons, and pest and disease dynamics are

already exhibiting signs of disruption due to climate-related stressors. Without targeted adaptation strategies and region-specific policy responses, climate change may exacerbate existing structural vulnerabilities, contributing to rural depopulation and socioeconomic inequality [24–27].

Knowledge on the timing and nature of shifts in climatic patterns is crucial for assessing climate impacts and informing adaptation strategies, particularly in vulnerable regions like South East Europe. One of the primary challenges in understanding these evolving patterns lies in detecting the moment when structural changes appear in the climatic time series. CPD techniques offer a powerful statistical framework for identifying structural changes in climate-related time series. CPD helps to detect shifts in the average, variance, or distribution of precipitation data, which may signify alterations in climate regimes due to external forcing [28–31]. This is particularly relevant for agriculture, where changes in rainfall timing and intensity directly affect sowing dates, crop yields, irrigation requirements, and drought risk [32]. To contextualize these changes and assess their broader implications, the use of climatic and drought indices such as the De Martonne Aridity Index and the Standardized Precipitation Index (SPI) is essential.

Various approaches to CPD are known, with applications in time series analysis, signal processing, and network traffic control [33–36], medicine [37–39], hydrometeorology [40–43], and economics and finance [44,45]. A review of various techniques for CPD is presented in [46].

Aridity reflects a moisture deficit caused by low effective rainfall and high evaporation, influenced largely by temperature. Aridity indices quantify this dryness, helping to classify climates based on water availability. I_M is one of the most widely used indices due to its simplicity and effectiveness, combining precipitation and temperature into a single metric. These characteristics make it valuable for understanding spatial and temporal shifts in aridity and agricultural suitability zones [47]. It has been applied to address drought risk in studies from all over the world [48–53]. Given the warming trends across the SEE region and the sensitivity of flora, fauna, and crops to water availability, tracking shifts in this index can help to identify regions undergoing significant hydroclimatic stress. In this study, it is applied to assess long-term aridity trends during 1965–2019 in the Danube Delta, where increasing aridity can have serious ecological consequences.

Another key tool for evaluating the impact of these shifts on drought risk is SPI, a statistically robust drought indicator that uses historical precipitation data to quantify deviations from normal conditions. Its strength lies in its simplicity and its capacity to reflect both short-term meteorological droughts and long-term hydrological imbalances. Widely recognized for its ability to quantify meteorological drought across different timescales, it is particularly useful in assessing short-term and long-term drought patterns and their evolution under changing climatic conditions. These properties make it a critical tool for understanding how droughts affect planting, growing, and harvest seasons, key information for developing responsive agricultural management practices [54–57].

The Danube Delta, a UNESCO-protected wetland and a critical biodiversity hotspot, is highly sensitive to climate variability. Therefore, detecting modifications in climatic variables is essential, as even small shifts can produce ecosystem imbalances, affect freshwater habitats, and contribute to the degradation or loss of species. Moreover, no extended studies addressed the modifications in aridity in this area for a period covering more than five decades.

This study applies I_M, SPI, and CUSUM to a long-term monthly precipitation time series (1965–2019) from the Sulina hydrometeorological station in the DDBR, Romania. Whereas CPD is generally used for time series, we apply it to I_M and SPI series to better

assess the modifications in climate evolution. To our knowledge, this is the first time such an approach has been proposed.

Whereas most studies about Dobrogea (the region to which the Danube Delta belongs) address only the temperature and/or precipitation variations in some zones or the drought intensity, the integration of I_M, SPI, and CPD allows for a more nuanced understanding of climate variation, particularly in complex regions where microclimates and topography can strongly modulate climatic signals.

By evaluating the temporal evolution of drought utilizing I_M and SPI and identifying potential structural changes in these indices, this research provides insights into local climate dynamics and supports regional adaptation planning. The methodology proposed here offers a scalable approach for monitoring climate impacts and can be applied regardless of the study zone. CUSUM analysis applied not only to the precipitation series but also to I_M and SPI provides complementary perspectives on climate variability and possible impacts on the ecosystem of the Danube Delta. By identifying historical shifts and current trends, these tools support targeted adaptation measures, including water management and regional planning.

2. Methodology and Data Series

2.1. Methodology

Most articles addressing climate evolution in the study area analyzed either the existence of a linear long-term trend in the data series or aridity using an aridity index. However, none of them combined these aspects with CPD, nor did they assess climatic variability by applying CPD to aridity indices. Therefore, we combined all of these approaches in our research, which are the following.

I. *Basic statistical analysis*

This stage involved computing the basic statistics, testing the normality hypothesis using the Shapiro–Wilk test [58], and detecting aberrant values using the interquartile range method (IQRM) [59]. According to IQRM, all values outside the interval $[Q_1 - 1.5IQR,\ Q_3 + 1.5IQR\ ]$ are considered outliers. Q_1, Q_3, and $IQR = Q_3 - Q_1$ are the first and third quantiles and the interquartile range, respectively. In this study, we extended the interval, replacing 1.5 in the formula above with 3 (to be more conservative, a larger factor like 3 results in fewer data points being classified as outliers compared to using 1.5).

II. *Perform CPD using the CUSUM change point algorithm*

The results are compared with those of classical algorithms—Pettitt [60], Buishand [61], and Lee & Heghinian [62]—which detect only the dominant change point (CP), and the segmentation method of Hubert [63] for determining multiple CPs.

For an input series $(Y_i)_{i=\overline{1,n}}$, the CUSUM procedure involves the following steps: computing the series mean, calculating the cumulative sums, identifying the amplitude of the CUSUM series, bootstrapping the original series, and comparing the amplitude of the original series with that of the bootstrapped series. If the amplitude of the original series is lower than that of the bootstrapped one, the confidence level (CL) of the change occurrence is determined by their ratio [64], as follows:

$$CL(\%) = N_1/N \times 100 \quad (1)$$

where N and N_1 are the number of bootstrap samples and those that satisfy the condition, respectively. $CL > 90\%$ indicates a high probability of CP occurrence.

If the series has a high number of outliers, it could be appropriate to use the non-parametric CUSUM, even if the parametric procedure is robust to aberrant values. In

this procedure, $\overline{Y}$ is replaced by the median, *Me*, and the sums are computed using the signs 1, −1, or 0 depending on whether the recorded value is greater, smaller, or equal to *Me*, respectively.

III. *Compute I_M and determine the CPs in the (I_M) series*

I_M is a simple climatic indicator for assessing aridity, especially in relation to water availability and drought risk. It is particularly useful for semi-arid regions like Dobrogea and the Danube Delta, where understanding the balance between precipitation and temperature is essential for water resources and land management. It is calculated by [37]:

$$I_M = P/(T + 10) \quad (2)$$

where P and T are the precipitation [mm] and the average temperature [°C], respectively.

In the case of the annual index, the total precipitation and annual mean temperature are used, whereas for the monthly index, the monthly precipitation and mean monthly temperature are employed.

The region is classified as hyper-arid, arid, semi-arid, moderately arid, slightly arid, or moderately humid, respectively, if $0 \leq I_M < 5$, $5 \leq I_M < 15$, $15 \leq I_M < 24$, $24 \leq I_M < 30$, $30 \leq I_M < 35$, or $35 \leq I_M < 40$, respectively.

This index was chosen because it uses only precipitation and temperature data, applies at multiple scales, adjusts for cold climates, tracks seasonal and long-term aridity changes, and supports comparisons and water management [65,66].

After computing the I_M series at the monthly and annual range, we applied CUSUM to determine the existence of CPs. The existence of a monotonic trend on the detected segments was assessed using the Mann–Kendall test [67].

IV. *Compute SPI*

The stages of SPI computation are [68]:

- Compute the mean, standard deviation, and skewness of the precipitation series.
- Take the logarithm of the precipitation series, and fit a gamma distribution. The validation of this distribution was performed using the Anderson–Darling and Kolmogorov–Smirnov goodness-of-fit tests. Since the p-value was greater than 0.05 (the significance level) in both cases, the null hypothesis that the series follows a gamma distribution cannot be rejected [69].
- Build the Cumulative Distribution Function (CDF), G.
- Adjust the CDF to accommodate the argument null values, using the following formula:

$$H(x) = q + (1 - q)G(x) \quad (3)$$

where q is the probability that there are zeros in the data series.

- Transform H into a Gaussian standard distribution. The computed values represent SPI values.

The drought categories according to SPI are: extreme drought for −2.0 or below; severe drought for SPI from −1.5 to −1.99, moderate drought for values between −1.0 and −1.49, values between −0.99 and 0.99 indicate near-normal conditions, while positive values correspond to wet conditions ranging from moderately wet (1.0 to 1.49) to extremely wet (2.0 and above) [57].

CPD was also performed to determine if there were changes in the SPI pattern.

2.2. The Study Region and Data Series

The Danube Delta is part of Dobrogea, a region situated in Romania between the Danube River and the Black Sea. Geographically, the area lies approximately between 44°00′ N and 45°30′ N latitude and 28°00′ E and 29°45′ E longitude. The region is characterized by a diverse topography, ranging from the ancient Măcin Mountains (reaching elevations of ~467 m) in northern Dobrogea to the flat, low-lying landscapes of the Danube Delta, most of which lie just above sea level. Dobrogea (Figure 1) experiences a continental-temperate climate with semi-arid characteristics, particularly in the southern and central parts.

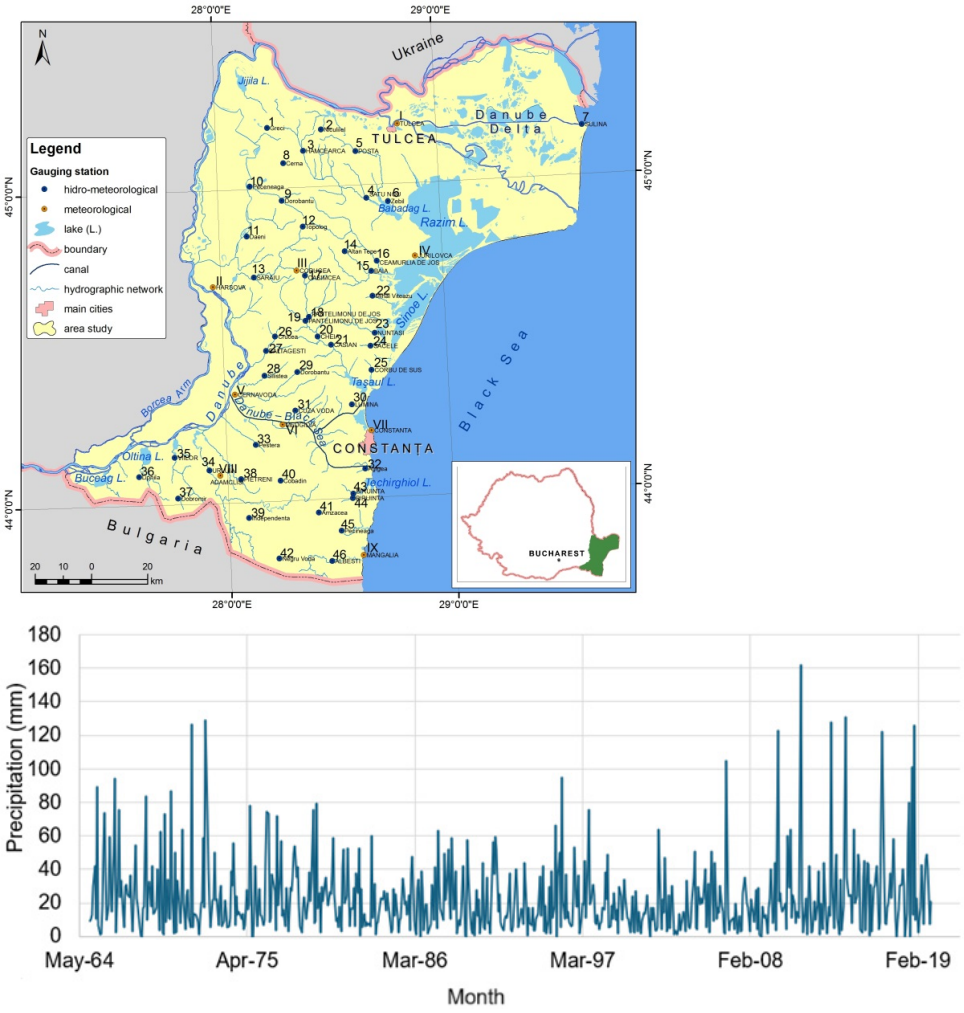

Figure 1. Map of Romania (**top**) and the Sulina monthly precipitation series (mm) (**bottom**).

The mean annual precipitation ranges between 350 mm and 450 mm, with most rainfall occurring during late spring and early summer. The region is prone to frequent droughts and marked interannual variability in precipitation, which significantly affects soil moisture, agricultural output, and hydrological processes [70].

Dobrogea experienced severe droughts in the years 2000–2001, 2007, 2011, 2012, 2015–2016, and 2019–2020, with the most critical impacts in 2012 and 2020, resulting from climate change and anthropogenic influences [71–80]. These events caused substantial agricultural and economic effects, particularly affecting the central, southern, and northwestern parts of the region due to acute water scarcity. For example, wheat yields fluctuated dramatically, ranging from as low as 296 kg/ha in 2003 to a peak of 3477 kg/ha in 2008, with the lowest production levels in 2001, 2002, 2007, and 2009. In the following decade,

the average wheat yield rose to 3713.4 kg/ha but still experienced drops during years such as 2010 and 2012–2014. The worst years for barley production were 2007, 2003, 2005, and 2000, followed by 2012, 2010, 2013, and 2019. Oat production dropped significantly in 2010, 2012, and 2013–2015. Maize yields were marked by below-average performance during 2012–2016, 2019, and 2010 [81]. Grape harvests have advanced by 12 days for Fetească Regală and 6 days for Fetească Neagră due to earlier ripening. Droughts (e.g., 2001 and 2020) and rainfall excesses (e.g., 2005 and 2010) frequently alternate, especially in July and August. These conditions have accelerated veraison and boosted sugar levels in grapes (~+40 g/L), resulting in higher alcohol content and sweeter wine types [82].

The Danube Delta Biosphere Reserve, a UNESCO World Heritage Site, covers more than 5800 km^2 and comprises a highly dynamic wetland system fed primarily by the Danube River's discharge, supplemented by local precipitation and influenced by Black Sea backwater effects. The delta's climate is slightly milder due to the maritime influence of the Black Sea, with a mean annual precipitation between 400 mm and 550 mm and a relatively high inter-seasonal variability. Precipitation in the DDBR plays a key role in maintaining hydrological connectivity, water quality, and biodiversity, particularly during periods of low river inflow [83]. Understanding precipitation patterns across the Dobrogea-Danube Delta system is critical for managing freshwater resources, mitigating drought risks, and preserving wetland functions in the face of ongoing climatic shifts and human-induced pressures, such as land use changes and upstream hydrological alterations.

The series the study consists of the monthly precipitation and temperature series spanning 1965 to 2019 from the Sulina meteorological station in the Danube Delta, Romania.

3. Results

3.1. Results of the Statistical Analysis

The monthly precipitation series $(Y_i)_{i=\overline{1660}}$ recorded in the DDBR from 1965 to 2019 had the following descriptive statistics: $\overline{Y} = 22.73$ mm, Me = 17.25 mm, min = 0.00 mm, max = 162.00 mm, standard deviation (stdev) = 21.95 mm, skewness coefficient (skew) = 2.25, and kurtosis (kurt) = 7.34. These results indicated that the series was right-skewed and leptokurtic, characterized by many relatively small precipitation values with high frequencies and high values with very low frequencies.

The Shapiro–Wilk test rejected the normality hypothesis. However, the series' normality was reached by a Box–Cox transformation, enabling the use of classical CPD techniques. The Buishand test rejected the null hypothesis that there is at least a CP, and the Pettitt and Lee & Heghinian tests indicated the dominant CP in August 1982 (month 212). Hubert's segmentation procedure provided the results presented Table 1.

Table 1. CPs detected by Hubert's procedure and the beginning and end of the time segments.

Beginning	End	Mean	Stdev
1	91	27.46	25.16
92	93	102.75	38.54
94	557	21.22	17.54
558	558	163.00	0.00
559	581	17.00	13.02
582	582	129.00	0.00
583	592	20.93	16.68
593	593	132.00	0.00
594	660	31.18	26.53

The segments formed by one or two months—[92, 93], 558, 582, 593—indicate the existence of aberrant values corresponding to the months August 1992 (month 92),

September 1992 (month 93), June 2013 (month 582), and May 2014 (month 593). They were also flagged as aberrant by IQRM. Given the high number of outliers (24 observations) identified by IQRM, we employed the non-parametric CUSUM test based on ranks to enhance the robustness of CPD in the monthly precipitation series. The CUSUM chart (Figure 2) delineated six distinct temporal segments in the series, separated by statistically significant change points at months 212 (August 1982), 421 (January 2000), 472 (April 2004), 497 (May 2006), and 533 (May 2009).

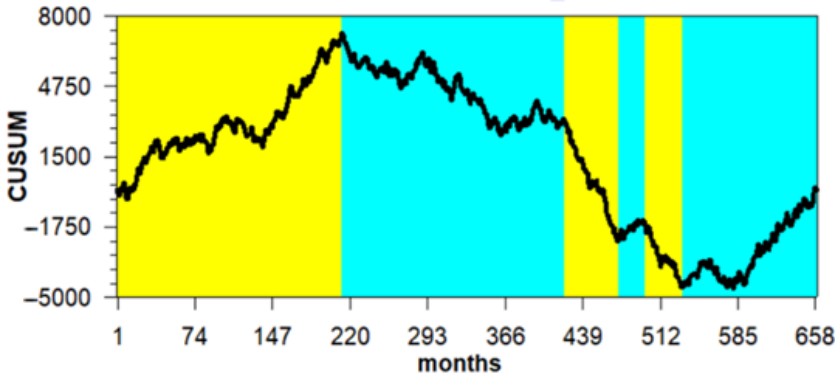

Figure 2. CUSUM chart for the monthly series (1965–2019). The periods delimited by CPs are represented in the CUSUM chart in different colors.

The first CP marked a substantial shift in the mean monthly precipitation, from 26.13 mm before August 1982 to 19.57 mm for the period from September 1982 to January 2000. The second CP delimited the previous period from February 2000 to April 2004, with an average of 12.30 mm. The existence of the second CP was also confirmed by the findings in [80,84,85]. The next change point delimitated the previous period from May 2004 to May 2006 (with an average of 22.58 mm). The fourth CP started a period with an average of 14.86 mm, until May 2009. The final change point corresponded to a renewed upward shift in CUSUM values, initiating a phase characterized by the highest variation in average (28.59 mm). This recent increase may reflect a potential regime shift, possibly driven by broader-scale climatic influences.

In Bulgaria, warming has been documented since the mid-1980s, with 2007 being recorded as the hottest year from 1961 to 1990, experiencing temperatures 1.6 °C above the average. The years 2000 and 2009 were also ranked among the warmest in the country. However, over the past 10 years, total rainfall has increased, resulting in significant flooding. This pattern of climate variation is similar to that observed in the Dobrogea region of Romania, to which Sulina belongs [86].

To investigate whether there was a systematic trend in each of the subseries delimited by the CPs, the Mann–Kendall trend test was applied on each of them. The test did not reject the null hypothesis of randomness in any segment, indicating that there were no statistically significant monotonic trends within the sub-periods. Therefore, the observed changes were better interpreted as shifts in mean levels rather than persistent directional trends.

3.2. Results for the De Martonne Aridity Index

I_M was computed using the annual and monthly data series (Figure 3). According to it (Figure 3, left), most months fell under the hyper-arid category, the rest being classified as arid: January of 1966 and 1968; December of 1966, 1968, and 2009; February of 1971, 1986, and 2003; November of 1965 and 2018; June 2011; and October 2016.

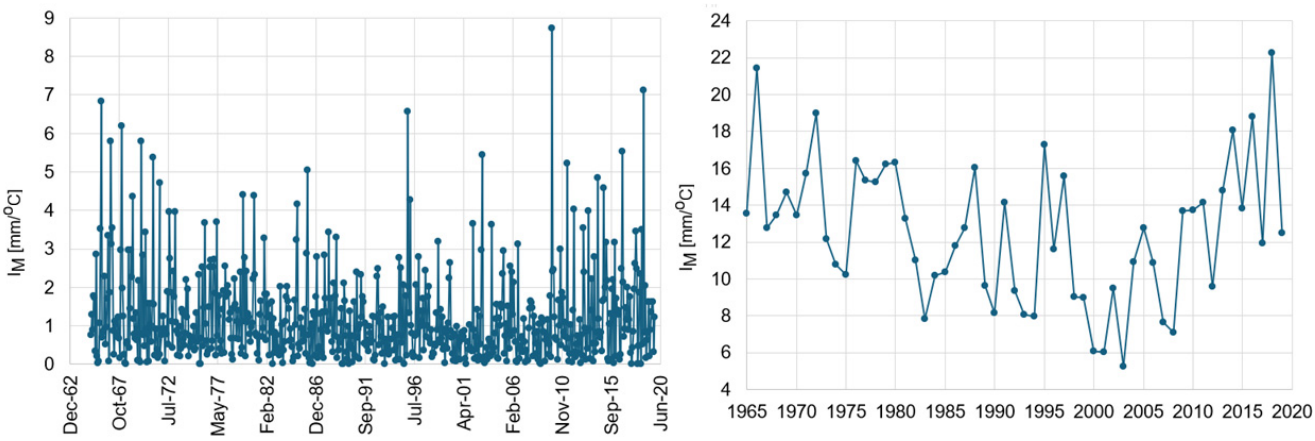

Figure 3. I_M for monthly (**left**) and annual (**right**) scales.

On an annual scale (Figure 3, right), I_M ranged from 5.26 to 22.25 mm/°C. The years 1966, 1971, 1972, 1976–1980, 1988, 1995, 1997, 2014, 2016, and 2018 were classified as semi-arid, while the remaining years were classified as arid. These findings were similar to those in [87], which indicated the highest water deficit in the Danube Delta compared to the rest of Romania, especially during summer and the maize-growing season. Notably, after 2013, the index revealed an alternation between arid and semi-arid conditions, suggesting increased interannual variability in precipitation and temperature.

The classical CPD methods identified August 1982 as a CP in the monthly I_M series, whereas CUSUM (Figure 4a) detected multiple CPs: September 1982, April 2000, January 2004, and May 2014.

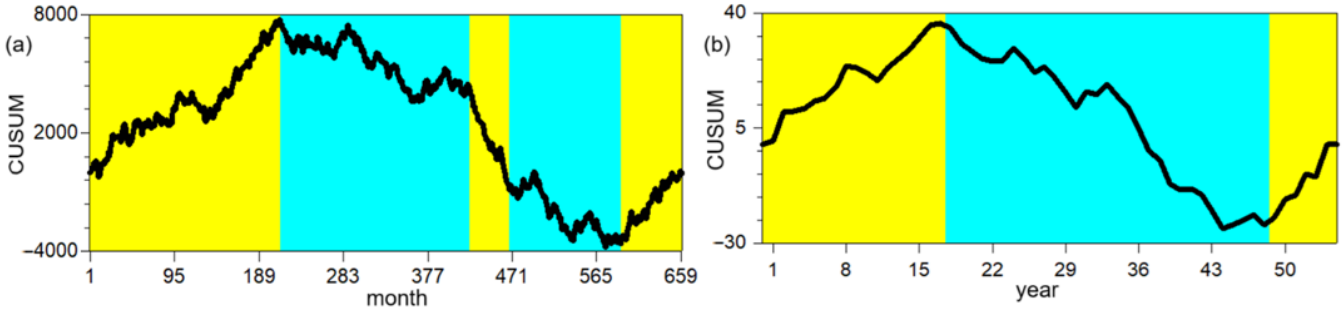

Figure 4. CUSUM for monthly (**a**) and annual (**b**) I_M.

The slight lag in the detection of the first three CPs, compared to those found in the raw precipitation series, and the highly similar CUSUM patterns observed for both precipitation and I_M series at the monthly level (Figure 2) suggested that precipitation (the numerator in Equation (2)) plays a dominant role with respect to temperature in shaping the variability of I_M.

The CPD methods identified the CPs in the annual I_M series at years 17 (Pettitt), 16 (Lee & Heghinian), 18, and 49 (Hubert and CUSUM), indicating a modification around 1982 (year 18) (Figure 4b). This supports the presence of a prominent shift in aridity index variation during that period. Additionally, both the Hubert segmentation and CUSUM test detected a second CP in 2013 (year 49), suggesting a more recent alteration in the aridity regime. The CPs with the confidence intervals, confidence levels, and average values in each segment for the monthly and annual I_M series are presented in Table 2.

Table 2. CPs detected by CUSUM procedure and the beginning and end of the time segments.

Month	Confidence Interval	Confidence Level	From	To	Year	Confidence Interval	Confidence Level	From	To
213	(57, 359)	90%	1.3665	1.0265	18	(14, 26)	100%	14.701	10.550
424	(348, 444)	93%	1.0265	0.6953	49	(44, 52)	96%	10.550	16.017
469	(448, 544)	98%	0.6953	1.0807					
593	(505, 646)	90%	1.0807	1.4994					

3.3. Results for SPI

The SPI values at 1 month (SPI-1) and SPI values at 12 months (SPI-12) are presented in Figure 5, and are contained in Table 2. In Figure 5 (top), the black horizontal lines indicate the limits of the normal precipitation regime. The region between the upper black line and the upper red line delimits the moderately and very wet regime. The zone above the upper red line shows the extremely wet periods. Similarly, the zone between the lower black line and the lower red line represents moderately to very high drought. Periods with extreme drought are indicated by values below the lower red line.

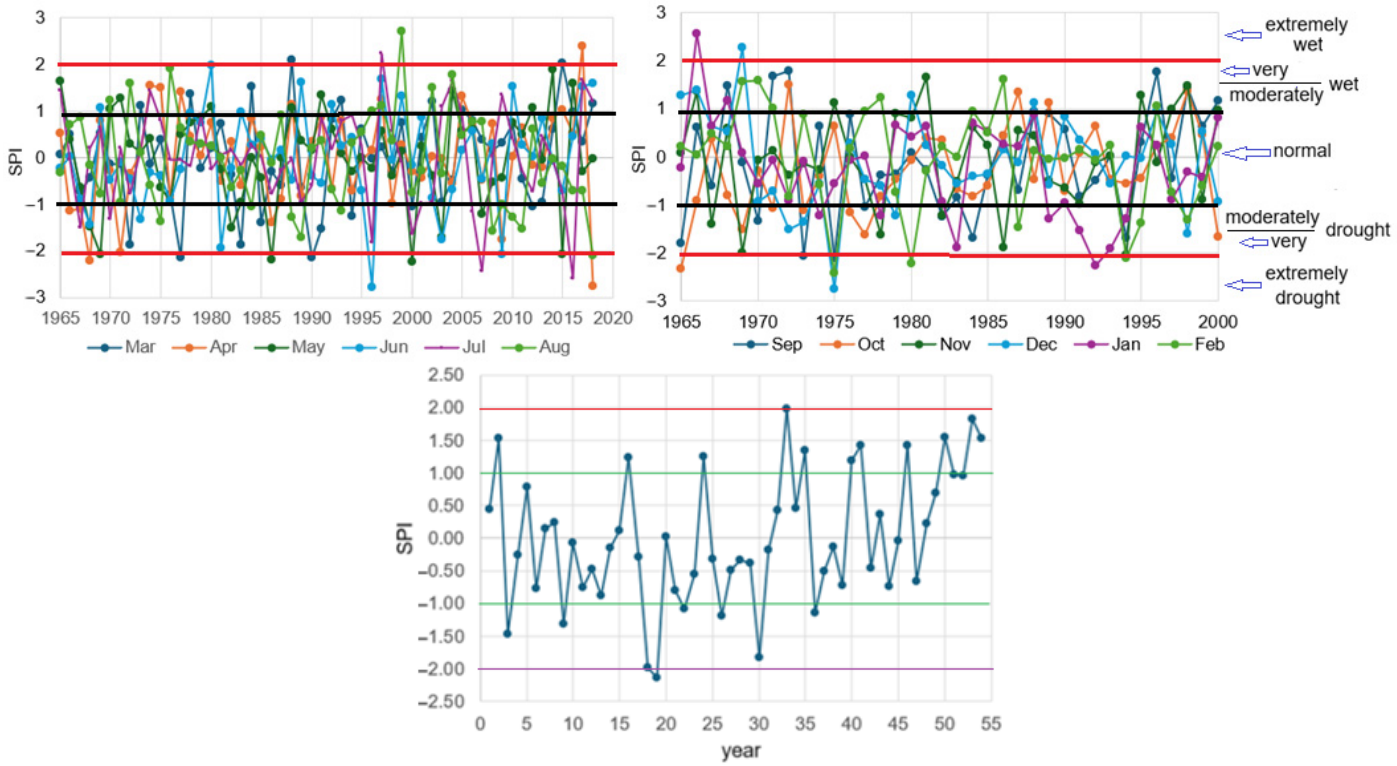

Figure 5. (**top left**) The SPI-1 chart for spring and summer months; (**top right**) the SPI-1 chart for autumn and winter months; and (**bottom**) the SPI-12 chart. The green lines mark the thresholds of the normal precipitation regime. The area between these green lines represents periods with near-normal precipitation. The red line indicates the upper threshold for the extremely dry category, while the purple line denotes the lower threshold for the extremely wet category.

SPI-1 (Table 3) indicated a predominantly normal precipitation regime, punctuated by alternating moderately wet and moderately dry periods. SPI-1 indicated that only a few very wet periods were noticed after 2013, especially in spring and summer. Over the recent decade, a pattern of alternating normal, very wet, and wet periods became evident. Notable intensifications in both wet and dry extremes were observed toward the end of the study period, especially in the summer and spring months.

Table 3. SPI-1.

Year	Jan	Feb	Mar	Apr	May	Jun	Jul	Aug	Sep	Oct	Nov	Dec
1965	−0.23	0.22	0.07	0.51	1.64	−0.23	1.42	−0.33	−1.79	−2.32	0.09	1.27
1966	2.57	0.04	0.49	−1.15	0.39	0.03	−0.04	0.71	0.62	−0.92	1.37	1.39
1967	0.63	0.48	−0.73	−1.09	−0.63	−0.89	−1.51	0.86	−0.60	0.38	−1.40	0.65
1968	1.18	0.21	−0.43	−2.21	−1.49	−1.44	0.20	−0.17	1.48	−0.80	0.59	0.52
1969	0.09	1.57	0.52	0.80	−2.08	1.06	0.64	−0.78	−0.12	−1.50	−1.99	2.27
1970	−0.55	1.59	−0.13	−0.27	1.05	−0.49	−1.32	1.22	−1.33	−0.29	−0.08	−0.94
1971	−0.07	1.01	−0.14	−2.02	1.28	−0.09	0.21	−0.95	1.68	−1.06	0.13	−0.72
1972	−0.90	−0.82	−1.86	−0.34	0.30	−0.45	−0.77	1.59	1.80	1.51	−0.37	−1.50
1973	−0.10	0.89	1.11	0.11	0.10	−1.33	0.17	0.11	−2.05	−1.12	−0.13	−1.35
1974	−1.23	−0.57	−0.15	1.54	0.41	−0.33	1.43	−0.59	0.65	−0.40	−0.26	−0.55
1975	−0.56	−2.41	0.39	1.50	−0.65	−0.40	0.80	−1.37	−2.10	0.65	1.12	−2.75
1976	−0.07	0.18	−0.80	−0.90	−0.94	−0.94	−0.05	1.91	0.88	−1.15	0.00	0.28
1977	0.02	0.94	−2.14	1.41	0.50	−0.26	−0.04	0.64	−1.04	−1.61	−0.47	−0.46
1978	−1.22	1.23	1.36	0.46	0.75	0.96	−0.19	0.34	−0.37	−0.83	−1.62	−0.59
1979	0.67	−0.73	−0.24	0.05	0.85	0.74	0.91	0.29	−0.36	−0.47	0.91	−1.23
1980	0.41	−2.22	0.21	0.75	1.09	1.98	−0.26	0.24	0.08	−0.06	0.82	1.27
1981	0.65	−0.28	0.73	−0.51	−0.26	−1.93	0.07	0.00	−0.26	0.40	1.66	0.24
1982	−0.94	0.22	−0.36	0.34	−1.51	−0.22	0.16	−0.65	−1.24	0.36	−1.23	−0.18
1983	−1.89	0.00	−1.88	−0.59	−0.95	0.97	−0.16	−0.28	−0.85	−0.66	−0.52	−0.55
1984	0.70	0.95	1.51	0.83	−0.01	0.27	0.28	−1.04	−1.69	−0.83	0.62	−0.40
1985	0.53	0.51	−1.39	0.23	−0.43	0.40	0.01	0.48	−0.38	−0.61	0.24	−0.35
1986	0.27	1.62	−0.31	−1.40	−2.18	−0.06	−0.77	−0.12	0.43	0.45	−1.89	0.15
1987	0.22	−1.47	−0.60	−0.88	−0.01	0.15	−0.28	0.91	−0.69	1.35	0.54	−0.12
1988	0.89	0.12	2.10	1.14	1.06	−0.48	−0.03	−1.28	0.94	−0.47	0.44	1.12
1989	−1.28	−0.05	−0.65	−0.83	0.37	1.62	−0.95	−1.70	0.91	1.13	−0.50	−0.57
1990	−0.96	−0.02	−2.14	0.33	0.16	−0.38	−0.59	0.20	0.58	−0.70	−0.65	0.83
1991	−1.54	0.15	−1.53	0.85	1.34	−0.56	0.85	0.35	−0.83	0.09	−0.97	0.36
1992	−2.27	−0.06	0.82	−0.66	0.61	1.14	0.18	−0.69	−0.50	0.63	−0.12	0.06
1993	−1.91	0.25	1.23	0.79	0.09	0.24	0.80	−1.14	0.02	−0.47	0.02	−0.55
1994	−1.28	−2.11	−1.26	−0.70	−0.30	0.42	0.90	0.31	−1.69	−0.55	−2.03	0.01
1995	0.61	−1.37	0.61	−0.06	−0.01	−0.71	0.26	0.54	0.30	−0.44	1.28	−0.02
1996	0.25	1.06	−0.02	0.16	−0.22	−2.79	−1.83	1.00	1.77	0.24	−0.12	0.94
1997	−0.89	−0.73	0.23	1.25	0.56	1.67	2.22	1.11	−0.45	0.39	0.99	0.26
1998	−0.31	−1.30	−0.29	−0.99	−0.38	−0.06	0.56	0.37	1.43	1.36	1.47	−1.60
1999	−0.42	−0.61	0.74	0.28	0.13	1.32	−0.09	2.70	0.63	0.46	−0.89	0.53
2000	0.81	0.21	−1.06	−0.29	−2.24	−0.17	−1.64	−0.76	1.18	−1.66	0.96	−0.93
2001	−1.59	−0.01	0.42	−0.44	0.25	0.86	−0.98	−0.28	0.54	0.07	0.68	−0.03
2002	−0.72	−0.12	1.20	0.01	−0.40	−0.86	−0.97	1.50	−0.24	1.50	0.53	−0.45
2003	0.75	0.54	−0.97	−0.03	−1.70	−1.76	1.09	−0.35	0.24	0.43	−0.63	0.24
2004	0.70	−0.41	−0.49	−0.56	1.44	−0.69	1.63	1.78	0.15	0.15	0.34	0.50
2005	0.92	0.74	1.02	1.31	0.56	0.15	0.93	0.47	0.48	−0.90	1.46	0.12
2006	0.03	−0.55	0.79	0.73	0.61	0.57	−1.16	0.78	0.63	−1.58	−0.99	−0.55
2007	0.03	−0.20	0.38	−0.47	−1.21	−0.45	−2.44	0.76	0.57	1.42	1.16	1.51
2008	−0.64	−1.35	0.15	0.73	−0.53	0.29	0.03	−1.57	1.07	−0.47	−0.73	0.44
2009	0.79	−0.20	0.31	−1.75	−0.44	−2.08	1.34	−1.01	0.24	0.48	−1.07	1.69
2010	0.55	1.42	0.73	0.03	0.75	1.52	0.41	−1.28	0.07	1.27	−0.42	1.16
2011	1.19	0.09	−0.46	0.64	0.50	0.27	−0.28	−1.53	0.02	0.02	−1.69	0.02
2012	1.77	−0.20	−1.06	−0.16	1.06	0.01	−0.73	0.60	−0.50	0.24	−0.79	1.38
2013	1.37	−0.05	−0.95	−0.20	−0.06	0.83	0.45	−0.56	1.24	1.77	−0.79	−1.72

Table 3. *Cont.*

Year	Jan	Feb	Mar	Apr	May	Jun	Jul	Aug	Sep	Oct	Nov	Dec
2014	1.19	−0.20	0.61	0.83	1.89	−0.07	−0.05	−0.02	−0.16	0.48	1.41	1.53
2015	−0.27	1.55	2.02	1.01	−2.07	−0.71	−0.73	−0.19	−0.01	1.93	1.83	−1.87
2016	1.52	−1.93	0.98	0.53	1.60	0.46	−2.59	−0.70	1.01	1.60	0.06	−1.20
2017	0.21	0.34	0.34	2.39	−0.30	1.52	1.65	−0.71	−2.31	1.60	0.35	0.41
2018	0.37	2.19	1.16	−2.75	−0.02	1.60	1.20	−2.09	0.38	−0.71	1.34	0.21

Legend: dark blue—extremely wet, blue—very wet, light blue—moderately wet, green—normal, yellow—moderate drought, orange—severe drought, red—extreme drought.

The SPI values computed at the annual scale (Figure 5 bottom) further suggested that, overall, the last decade has been dominated by normal to wet precipitation regimes. The CUSUM analysis indicated a single CP in SPI-1 in August 1996 from an average of −0.1103 to 0.1624. It also detected a significant change point in 2013 (from an average of −0.1563 to 1.2533), aligning with a similar shift detected in the I_M annual series, which reinforces the evidence of a climatic regime change during this period.

To complement the analysis at various temporal scales, the SPI values at 3 and 6 months (SPI-3 and SPI-6) were also calculated (Figure 6).

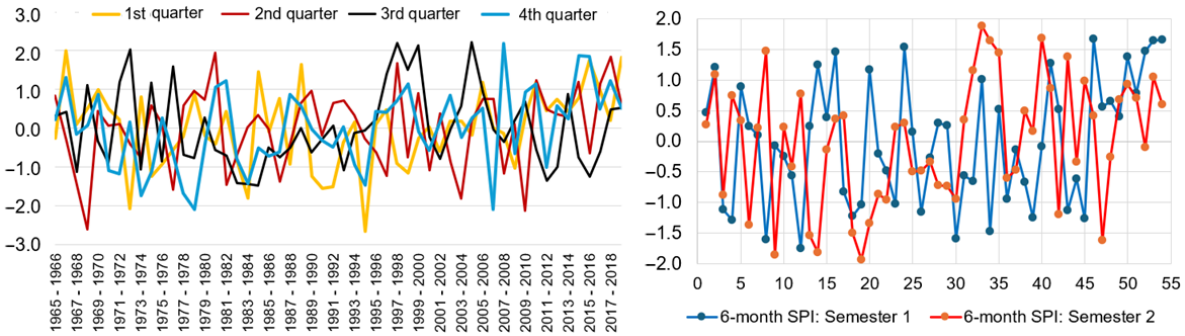

Figure 6. The charts of SPI-3 (**left**) and SPI–6 (**right**).

These indicators revealed notable seasonal variability. The most significant fluctuations occurred in the second quarter for SPI-3 and in the second semester for SPI-6, indicating periods of abrupt changes in precipitation patterns. Except for 10 instances, all SPI-3 values fell within the categories ranging from moderately dry to moderately wet. Similarly, all the values of SPI-6 also fell within these same categories for the entire period.

The CPA analysis found:

- A CP in SPI-3 during the first quarter and SPI-6 during the first semester of 2011.
- No CP in SPI-3 during the second quarter.
- Two CPs in SPI-3 during the third quarter of the years 1996 and 2000. Specifically, they showed transitions from normal to extreme wet or very wet to extreme wet periods, respectively.
- A CP in SPI-3 during the fourth quarter and SPI-6 during the second semester of 2000.
- All values of SPI-6 indicated a high variability in the precipitation regime, with a tendency toward very wet periods in the second semester in the last study years.

4. Discussion

In this study, we investigated climatic aridity using the De Martonne Aridity Index, detected and quantified meteorological drought using SPI, and identified abrupt changes in average precipitation and series of indices utilizing CUSUM. When used together, I_M and SPI offer complementary perspectives on climatic conditions because the first index

captures the long-term climatic balance between precipitation and temperature, whereas SPI reflects fluctuations in precipitation at various scales.

According to I_M, the climate in the DDBR is classified as arid to severely arid at a monthly scale, and semi-arid to arid on an annual scale. By contrast, SPI identified only a few periods of dryness but revealed significant variability in the precipitation regime, particularly after 2013, when wetter conditions became more frequent compared to the earlier periods.

Discrepancies between I_M and SPI—particularly when SPI indicates normal or wet conditions while I_M signals aridity—are common in drought assessments. This divergence arises primarily because I_M incorporates both temperature and precipitation, making it more sensitive to warming trends. As a result, even when rainfall remains stable or increases, rising temperatures can lead to I_M indicating more arid conditions. On the other hand, SPI is a probabilistic measure based solely on precipitation series over various timeframes. Therefore, periods of elevated temperatures and average rainfall may be classified as normal or wet by SPI, while I_M may still reflect severe aridity due to increasing temperatures.

Correlation analysis between the SPI-12 and annual I_M series provided a correlation coefficient of $r = 0.53$, with a p-value of 0.02. Even though r was not very high, it indicated an acceptable concordance between the classifications provided by SPI-12 and annual I_M. The complementary natures of I_M and SPI, and their combined use, provide a more robust foundation for climate risk and agricultural vulnerability assessments.

Change point analysis supported the hypothesis of shifts in aridity and precipitation regimes, indicating changes in the mean values of these parameters without clear evidence of modifications in their overall trend.

Deeper insights into previous studies on the European trend of climate change evolution and that at Sulina (and Dobrogea, in general) indicate the following.

- In the Dobrogea region, including Sulina, a modest warming trend was observed between 1960 and 1980, with a multi-station average annual mean increase of approximately 0.8 °C since the late 1990s [42,84,88]. After 1988, statistically significant increases in minimum and mean temperatures were recorded. Specifically, there was an average increase of around 0.7 °C at Sulina and neighboring stations, with minimum temperatures rising after approximately 1988 and mean temperatures increasing after around 1997 [89]. From 1961 to 2013, average annual temperatures fluctuated between 9.7 °C and 12.3 °C, with the most significant increases occurring in the latter decades. By comparison, European land temperatures rose by about 1.4 to 1.6 °C during the period from 2006 to 2015 relative to pre-industrial levels, highlighting Europe as one of the fastest-warming continents.
- In the winter and fall seasons, there has typically been a stronger increase in minimum (overnight) temperatures since 1988. Weather stations in Sulina and Dobrogea have recorded more significant rises in minimum temperature, suggesting milder winters. For the summer months, observational data reveal that maximum temperatures have risen by approximately 0.6 °C per decade in July and about 0.65 °C per decade in August at coastal and Danube Delta stations. Additionally, the number of days exceeding 30 °C has become more frequent between 1965 and 2005, particularly in July and August. This trend has heightened the risk of crop failure during extreme summer conditions, such as those experienced in 2000 [51,89].
- At Sulina, the annual precipitation decreased from approximately 281 mm during the period of 1961–1990 to about 229 mm in 1980–2009, resulting in a decline of over 50 mm across three decades. This brings the area below the global arid threshold of approximately 229 mm per year. Dry spells are becoming longer, and precipita-

tion intensity—measured by indices such as R95p and SDII—is increasing in parts of Dobrogea. Drought analyses conducted using the Standardized Precipitation-Evapotranspiration Index (SPEI) and the Composite Drought Index from 2001 to 2021 indicate that the period from 1991 to 2021 was the driest in Dobrogea since 1901. Severe and extreme drought occurrences peaked in the years 2011–2012, 2015, and 2020, impacting as much as 70% of the region [51,90].

- Heatwaves in Southern Romania have become longer, more frequent, and more intense since 1961, particularly after 1990. By contrast, cold spells have decreased in both frequency and severity. Additionally, the spring and autumn seasons are getting shorter, with extreme heat events increasingly extending into transitional months, such as late spring and early fall. This shift is noticeably altering the seasonal experience for daily life [91]. These findings are in concordance with the general trend in SSE, as presented in [13–19].

The results of this study are consistent with most of the above findings, as, for example those reported by Cheval et al. [88], Lungu et al. [51] (who analyzed aridity conditions in Dobrogea prior to 2011 and classified the region as semi-arid, though they did not address climatic variability specifically in the DDBR), Bădăluță et al. [92] (who used SPEI-3 and found that, between 1991 and 2021, severe droughts occurred in the southern Danube Delta and the frequency of extreme droughts increased across Dobrogea), and Bandoc and Prăvălie [93] (who detected a climatic water deficit at Sulina before 2009 and reported that the most severe droughts in continental Dobrogea occurred in 2011 and 2012). Our results are partially concordant with those of Serban and Maftei [80] for 2012, emphasizing the unique and evolving climatic pattern in the Danube Delta region.

5. Conclusions

This study assessed potential changes in precipitation patterns in Romania, with a specific emphasis on detecting CPs in long-term monthly rainfall data. The analysis was conducted using data from 1965 to 2019 recorded at the Sulina hydrometeorological station located in the DDBR—an ecologically sensitive area where climatic shifts can have far-reaching effects. Identifying change points within the precipitation series allowed for the detection of abrupt or gradual shifts in the rainfall regime, which can serve as indicators of climate variability. Such insights are critical for anticipating ecological responses and informing water management and conservation strategies in this unique and fragile ecosystem.

At the annual scale, I_M indicated a decrease in aridity in 2014, 2016, and 2018, in contrast to the severe aridity observed in most previous years. At the monthly scale, most records indicated severe aridity. The analysis of SPI-1, SPI-3, and SPI-6 revealed high variability in precipitation across different scales, with the most pronounced fluctuations in SPI-3 and SPI-6. Apart from previous studies, the present one enriched knowledge of the study area by addressing shifts in climate through nonparametric CUSUM, a method that has not been previously applied. By applying CPD to climatic datasets, researchers can gain a deeper understanding of the timing and nature of climatic shifts, thereby enhancing adaptive strategies and resilience planning. In this case, they revealed modifications in mean climate indicators, especially after 2013.

Effective strategies must be multidimensional, addressing the agricultural, hydrological, ecological, and infrastructural vulnerabilities of the region, while aligning with both national and European Union (EU) policy frameworks. The action directions include: (1) climate-smart agriculture, i.e., promoting drought-tolerant crop varieties and conservation agriculture practices (e.g., no-till farming, crop rotation, and organic mulching) to enhance soil moisture retention and reduce erosion; (2) water resource management, e.g., modernization of irrigation infrastructure and strategic water allocation, as well as imple-

menting drought early warning systems and regional water-sharing agreements; (3) coastal protection measures (e.g., vegetated barriers and dune reinforcement); and (4) land use planning to restrict development in high-risk floodplains, etc. [94–100].

The Danube Delta is highly susceptible to sea level rise, saltwater intrusion, and changes in river dynamics. Implementing ecosystem-based adaptation measures—such as wetland restoration, reforestation, and the establishment of buffer zones—can enhance biodiversity and provide natural protection against floods and droughts. It is essential to expand conservation efforts both within and around protected areas, along with initiatives that promote habitat connectivity, to safeguard migratory species and maintain wetland integrity in the face of changing climatic conditions [101].

Despite the ecological importance of the DDBR, significant gaps remain in understanding its climate evolution, particularly over the past two decades. While recent analyses, including the present study, offer valuable insights into changing patterns of aridity and precipitation, these findings should be further validated through extended research that will include other drought indices. Confirmatory studies using longer and higher-resolution climate records, additional drought and aridity indices, and improved spatial coverage are essential to establish the robustness of the observed changes.

A comprehensive database including other variables is also necessary better to detect the extent of extreme events in the region. Integrating remote sensing data with hydrological models and field-based observations could enhance the understanding of the complex interactions between climatic variability and the Delta's sensitive ecosystems.

Furthermore, applying a range of CPD methods alongside additional climate and drought indices would strengthen the robustness of the current findings. Such a multidisciplinary approach would provide a more comprehensive foundation for developing effective climate adaptation strategies, promoting sustainable water resource management, and informing conservation policies within the region.

Author Contributions: Conceptualization, A.B. and C.Ș.D.; methodology, A.B. and C.Ș.D.; software, A.B.; validation, C.Ș.D.; formal analysis, A.B. and C.Ș.D.; investigation, A.B. and C.Ș.D.; resources, A.B.; data curation, A.B.; writing—original draft preparation, A.B. and C.Ș.D.; writing—review and editing, A.B.; visualization, A.B.; supervision, A.B.; project administration, A.B.; funding acquisition, C.Ș.D. All authors have read and agreed to the published version of the manuscript.

Funding: This research received no external funding.

Data Availability Statement: Data are freely available to download from European Climate Assessment & Data: https://www.ecad.eu/dailydata/index.php (accessed on 1 June 2025).

Conflicts of Interest: The authors declare no conflicts of interest.

Abbreviations

The following abbreviations are used in this manuscript:

CP	Change Point
CPD	Change Point Detection
CUSUM	Cumulative Sum
DDBR	Danube Delta Biosphere Reserve
I_M	De Martonne Aridity Index
IQRM	Interquartile Range Method
PDSI	Palmer Drought Severity Index
SEE	South East Europe
SPI	Standardized Precipitation Index

References

1. Kundzewicz, Z.W. Climate change impacts on the hydrological cycle. *Ecohydrol. Hydrobiol.* **2008**, *8*, 195–203. [CrossRef]
2. Hamder, J.; Honda, Y.; Kundzewicz, Z.W. Changes in Impacts of Climate Extremes: Human Systems and Ecosystems. Available online: https://www.ipcc.ch/site/assets/uploads/2018/03/SREX-Chap4_FINAL-1.pdf (accessed on 3 June 2025).
3. Ma, J.; Zhou, L.; Foltz, R.; Qu, X.; Ying, J.; Tokinaga, H.; Mechoso, C.R.; Li, J.; Gu, X. Hydrological cycle changes under global warming and their effects on multiscale climate variability. *Ann. N. Y. Acad. Sci.* **2020**, *1472*, 21–48. [CrossRef] [PubMed]
4. OBSERVER: Copernicus Climate Change Service Tracks Record Atmospheric Moisture and Sea Surface Temperatures in 2024. Available online: https://www.copernicus.eu/en/news/news/observer-copernicus-climate-change-service-tracks-record-atmospheric-moisture-and-sea (accessed on 14 March 2025).
5. Luo, Y.; Wang, L.; Hu, C.; Hao, L.; Sun, G. Changing Extreme Precipitation Patterns in Nepal Over 1971–2015. *Earth Space Sci.* **2024**, *11*, e2024EA003563. [CrossRef]
6. Wang, B.; Luo, X.; Yang, Y.-M.; Liu, J. Historical change of El Niño properties sheds light on future changes of extreme El Niño. *Proc. Nat. Acad. Sci. USA* **2019**, *116*, 22512–22517. [CrossRef] [PubMed]
7. Jiu, L.; Song, M.; Zhu, Z.; Horton, R.M.; Hu, Y.; Xie, S.-P. Arctic sea-ice loss is projected to lead to more frequent strong El Niño events. *Nat. Commun.* **2022**, *13*, 4952. [CrossRef]
8. McPhaden, M.J. El Nino and La Niña: Causes and Global Consequences. Available online: https://www.pmel.noaa.gov/gtmba/files/PDF/pubs/ElNinoLaNina.pdf (accessed on 1 June 2025).
9. Assessment of El Niño-Associated Risks: The Step-Wise Process. Available online: https://www.unescap.org/sites/default/files/FINAL_El%20Nino%20Methodology.pdf (accessed on 1 June 2025).
10. Bărbulescu, A. Modeling the greenhouse gases data series in Europe during 1990–2021. *Toxics* **2023**, *11*, 726. [CrossRef]
11. Antonescu, N.N.; Stănescu, D.-P.; Calotă, R. CO_2 Emissions Reduction through Increasing H_2 Participation in Gaseous Combustible—Condensing Boilers Functional Response. *Appl. Sci.* **2022**, *12*, 3831. [CrossRef]
12. Bărbulescu, A. Modeling Greenhouse Gas Emissions from Agriculture. *Atmosphere* **2025**, *16*, 295. [CrossRef]
13. IPCC. *Climate Change 2023: Synthesis Report. Contribution of Working Groups I, II and III to the Sixth Assessment Report of the Intergovernmental Panel on Climate Change*; IPCC: Geneva, Switzerland, 2023.
14. South East European Climate Change Center. Available online: http://www.seevccc.rs/?p=18 (accessed on 15 July 2025).
15. Spinoni, J.; Vogt, J.V.; Barbosa, P. European drought climatologies and trends based on a multi-indicator approach. *Glob. Planet. Change* **2015**, *127*, 50–57. [CrossRef]
16. Bulgaria. Climate Change. Available online: https://www.climatechangepost.com/countries/bulgaria/climate-change/ (accessed on 15 July 2025).
17. Nojarov, P. Genetic climatic regionalization of the Balkan Peninsula using cluster analysis. *J. Geogr. Sci.* **2017**, *27*, 43–61. [CrossRef]
18. Kostopoulou, E.; Giannakopoulos, C. Projected Changes in Extreme Wet and Dry Conditions in Greece. *Climate* **2023**, *11*, 49. [CrossRef]
19. Noto, L.V.; Cipolla, G.; Pumo, D.; Francipane, A. Climate Change in the Mediterranean Basin (Part II): A Review of Challenges and Uncertainties in Climate Change Modeling and Impact Analyses. *Water Resour. Manag.* **2023**, *37*, 2307–2323. [CrossRef] [PubMed]
20. Popescu, C.; Bărbulescu, A. Flooding simulation at the confluence between the Strâmba and Aluniș Rivers in the Vărbilău Catchment, in Romania. *Rom. Rep. Phys.* **2025**, *77*, 705. [CrossRef]
21. Mimikou, M.A.; Baltas, E.A. Assessment of Climate Change Impacts in Greece: A General Overview. *Am. J. Clim. Change* **2013**, *2*, 29099. [CrossRef]
22. Ju, X.; Li, W.; Li, j.; He, L.; Mao, J.; Han, L. Future climate change and urban growth together affect surface runoff in a large-scale urban agglomeration. *Sustain. Cities Soc.* **2023**, *99*, 104970. [CrossRef]
23. Song, Y.H.; Chung, E.-S.; Ayugi, B.O. CMIP6 GCMs projected future Koppen-Geiger climate zones on a global scale. *Earth's Future* **2025**, *13*, e2023EF004401. [CrossRef]
24. FAO. *Agricultural Transformation in Europe and Central Asia: Regional Synthesis Report*; Food and Agriculture Organization: Rome, Italy, 2022.
25. Županić, F.Ž.; Radić, D.; Podbregar, I. Climate change and agriculture management: Western Balkan region analysis. *Energy Sustain. Soc.* **2021**, *11*, 51. [CrossRef]
26. Filho, W.L.; Trbic, G.; Filipovic, D. *Climate Change Adaptation in the Agriculture of South-East Europe: Challenges and Policy Options*; Springer: Cham, Switzerland, 2018.
27. Ward, C.J.; Cope, M.R.; Wilson, D.R.; Muirbrook, K.A.; Poff, J.M. Powerless in a Western US Energy Town: Exploring Challenges to Socially Sustainable Rural Development. *Sustainability* **2020**, *12*, 8426. [CrossRef]
28. Reeves, J.; Chen, J.; Wang, X.; Lund, R.; Lu, Q.Q. A Review and Comparison of Changepoint Detection Techniques for Climate Data. *J. Appl. Meteor. Climatol.* **2007**, *46*, 900–915. [CrossRef]

29. Xie, P.; Gu, H.; Sang, Y.-F.; Wu, Z.; Singh, V.P. Comparison of different methods for detecting change points in hydroclimatic time series. *J. Hydrol.* **2019**, *577*, 123973. [CrossRef]
30. Rwema, M.; Sylla, M.B.; Safari, B.; Roinen, B.; Laine, M. Trend analysis and change point detection in precipitation time series over the Eastern Province of Rwanda during 1981–2021. *Theor. Appl. Climatol.* **2025**, *156*, 98. [CrossRef]
31. Liu, M.; Liu, P.; Guo, Y.; Wang, Y.; Geng, X.; Nie, Z.; Yu, Y. Change-Point Analysis of Precipitation and Drought Extremes in China over the Past 50 Years. *Atmosphere* **2020**, *11*, 11. [CrossRef]
32. Tomé, A.R.; Miranda, P.M.A. Piecewise linear fitting and trend changing points of climate parameters. *Geophys. Res. Lett.* **2004**, *31*, L02207. [CrossRef]
33. Darkhovsky, B.S.; Brodsky, B.E. *Nonparametric Methods in Change Point Problems*; Springer: Dordrecht, The Netherlands, 1993.
34. Jandhyala, S.; Fotopoulos, V.; Macneill, I.; Liu, P. Inference for single and multiple change-points in time series. *J. Time Ser. Anal.* **2013**, *34*, 423–446. [CrossRef]
35. Truong, C.; Oudre, L.; Vayatis, N. Selective review of offline change point detection methods. *Signal Proc.* **2020**, *167*, 107299. [CrossRef]
36. Lung-Yut-Fong, A.; Lévy-Leduc, C.; Cappé, O. Distributed detection/localization of change-points in high-dimensional network traffic data. *Stat. Comput.* **2012**, *22*, 485–496. [CrossRef]
37. Liu, S.; Wright, A.; Hauskrecht, M. Change-point detection method for clinical decision support system rule monitoring. *Artif. Intell. Med.* **2018**, *91*, 49–56. [CrossRef]
38. Chen, G.; Lu, G.; Shang, W.; Xie, Z. Automated Change-Point Detection of EEG Signals Based on Structural Time-Series Analysis. *IEEE Access* **2019**, *7*, 180168–180180. [CrossRef]
39. Yang, P.; Dumont, G.; Ansermino, J.M. Adaptive change detection in heart rate trend monitoring in anesthetized children. *IEEE Trans. Biomed. Eng.* **2006**, *53*, 2211–2219. [CrossRef]
40. Shi, X.; Beaulieu, C.; Killick, R.; Lund, R. Changepoint Detection: An Analysis of the Central England Temperature Series. *J. Clim.* **2022**, *35*, 6329–6342. [CrossRef]
41. Getahun, Y.S.; Li, M.-H.; Pun, I.-F. Trend and change-point detection analyses of rainfall and temperature over the Awash River basin of Ethiopia. *Heliyon* **2021**, *7*, e08024. [CrossRef]
42. Bărbulescu, A.; Deguenon, J. Change point detection and models for precipitation evolution. Case study. *Rom. J. Phys.* **2014**, *59*, 590–600.
43. Monteiro, M.; Costa, M. Change Point Detection by State Space Modeling of Long-Term Air Temperature Series in Europe. *Stats* **2023**, *6*, 113–130. [CrossRef]
44. Musaev, A.; Grigoriev, D.; Kolosov, M. Adaptive algorithms for change point detection in financial time series. *AIMS Math.* **2024**, *9*, 35238–35263. [CrossRef]
45. Manner, H.; Rodríguez, G.; Stöckler, F. A changepoint analysis of exchange rate and commodity price risks for Latin American stock markets. *Int. Rev. Econ. Financ.* **2024**, *89A*, 1385–1403. [CrossRef]
46. Aminikhanghahi, S.; Cook, D.J. A Survey of Methods for Time Series Change Point Detection. *Knowl. Inf. Syst.* **2017**, *51*, 339–367. [CrossRef]
47. De Martonne, E. Une nouvelle function climatologique: L'indice d'aridité. *Meteorologie* **1926**, *2*, 449–458.
48. Charalampopoulos, I.; Droulia, F.; Kokkoris, I.P.; Dimopoulos, P. Future Bioclimatic Change of Agricultural and Natural Areas in Central Europe: An Ultra-High-Resolution Analysis of the De Martonne Index. *Water* **2023**, *15*, 2563. [CrossRef]
49. Pellicone, G.; Caloiero, T.; Guagliardi, I. The De Martonne aridity index in Calabria (Southern Italy). *J. Maps* **2019**, *15*, 788–796. [CrossRef]
50. Mavrakis, A.; Papavasileiou, H. NDVI and E. de Martonne Indices in an Environmentally Stressed Area (Thriasio Plain—Greece). *Procedia Technol.* **2013**, *8*, 477–481. [CrossRef]
51. Lungu, M.; Panaitescu, L.; Niţă, S. Aridity, climatic risk phenomenon in Dobrudja. *Present. Environ. Sustain. Dev.* **2011**, *5*, 179–190.
52. Gebremedhin, M.A.; Abraha, A.Z.; Fenta, A.A. Changes in future climate indices using Statistical Downscaling Model in the upper Baro basin of Ethiopia. *Theor. Appl. Climatol.* **2018**, *133*, 39–46. [CrossRef]
53. Moral, F.J.; Rebollo, F.J.; Paniagua, L.L.; García-Martín, A.; Honorio, F. Spatial distribution and comparison of aridity indices in Extremadura, southwestern Spain. *Theor. Appl. Climatol.* **2016**, *126*, 801–814. [CrossRef]
54. Naresh Kumar, M.; Murthy, C.S.; Sesha Sai, M.V.R.; Roy, P.S. On the use of Standardized Precipitation Index (SPI) for drought intensity assessment. *Meteorol. Appl.* **2009**, *16*, 381–389. [CrossRef]
55. Tsesmelis, D.E.; Leveidioti, I.; Karavitis, C.A.; Kalogeropoulos, K.; Vasilakou, C.G.; Tsatsaris, A.; Zervas, E. Spatiotemporal Application of the Standardized Precipitation Index (SPI) in the Eastern Mediterranean. *Climate* **2023**, *11*, 95. [CrossRef]
56. Maftei, C.E.; Bărbulescu, A.; Osman, A. Assessment of the drought risk in Constanța County, Romania. *Atmosphere* **2024**, *15*, 1281. [CrossRef]
57. Standardized Precipitation Index (SPI). Available online: https://climatedataguide.ucar.edu/climate-data/standardized-precipitation-index-spi#:~:text=The%20Standardized%20Precipitation%20Index%20(SPI,to%20groundwater%20and%20reservoir%20storage (accessed on 3 June 2025).

58. Shapiro, S.S.; Wilk, M.B. An analysis of variance test for normality (complete samples). *Biometrika* **1965**, *52*, 591–611. [CrossRef]
59. Aakash, R. Outlier Detection and Treatment: Z-score, IQR, and Robust Methods. Available online: https://medium.com/@aakash013/outlier-detection-treatment-z-score-iqr-and-robust-methods-398c99450ff3 (accessed on 3 June 2025).
60. Pettitt, A.N. A non-parametric approach to the change point problem. *J. R. Stat. Soc. Ser. C Appl. Stat.* **1979**, *28*, 126–135. [CrossRef]
61. Buishand, T.A. Tests for detecting a shift in the mean of hydrological time series. *J. Hydrol.* **1984**, *73*, 51–69. [CrossRef]
62. Lee, A.F.S.; Heghinian, S.M. A Shift of the Mean Level in a Sequence of Independent Normal Random Variables—A Bayesian Approach. *Technometrics* **1977**, *19*, 503–506. [CrossRef]
63. Hubert, P. Segmentation Procedure as a Tool for Discrete Modeling of Hydro-Meteorological Regimes. *Stoch. Environ. Res. Risk Assess.* **2000**, *14*, 297–304. [CrossRef]
64. Taylor, W.A. Change-Point Analysis: A Powerful New Tool for Detecting Changes. 2000. Available online: https://variation.com/wp-content/uploads/change-point-analyzer/change-point-analysis-a-powerful-new-tool-for-detecting-changes.pdf (accessed on 4 June 2025).
65. Neniu, A.-I.; Vlăduț, A.Ș. The influence of climatic conditions on the forest vegetation within the Getic Subcarpatians—Oltenia sector. *Univ. Craiova Ser. Geogr.* **2020**, *21*, 5–18.
66. McKee, T.B.; Doesken, N.J.; Kleist, J. The relationship of drought frequency and duration to time scale. In Proceedings of the 8th Conference on Applied Climatology, Anaheim, CA, USA, 17–22 January 1993; pp. 179–184.
67. Kendall, M.G. *Rank Correlation Methods*, 4th ed.; Charles Griffin: London, UK, 1975.
68. Edwards, D.C.; McKee, T.B. Characteristics of 20th Century Drought in the United States at Multiple Times Scales. *Atmos. Sci. Pap.* **1997**, *634*, 1–30.
69. Ross, S.M. *Introduction to Probability and Statistica for Engineers and Scientists*; Elsevier: Amsterdam, The Netherlands, 2020.
70. Bărbulescu, A.; Dumitriu, C.S.; Maftei, C. On the Probable Maximum Precipitation Method. *Rom. J. Phys.* **2022**, *67*, 801.
71. Croitoru, A.-E.; Piticar, A.; Imbroane, A.M.; Burada, D.C. Spatiotemporal distribution of aridity indices based on temperature and precipitation in the extra-Carpathian regions of Romania. *Theor. Appl. Climatol.* **2013**, *112*, 597–607. [CrossRef]
72. Dumitrescu, A.; Bojariu, R.; Birsan, M.-V.; Marin, L.; Manea, A. Recent climatic changes in Romania from observational data (1961–2013). *Theor. Appl. Climatol.* **2015**, *122*, 111–119. [CrossRef]
73. Ionita, M.; Chelcea, S. Spatio-Temporal Variability of Seasonal Drought over the Dobrogea Region. In *Extreme Weather and Impacts of Climate Change on Water Resources in the Dobrogea Region*; IGI Global: Hershey, PA, USA, 2015; pp. 17–51.
74. Marin, L.; Birsan, M.-V.; Bojariu, R.; Dumitrescu, A.; Micu, D.M.; Manea, A. An overview of annual climatic changes in Romania: Trends in air temperature, precipitation, sunshine hours, cloud cover, relative humidity and wind speed during the 1961–2013 period. *Carpathian J. Earth Environ. Sci.* **2014**, *9*, 253–258.
75. Mateescu, E.; Smarandache, M.; Jeler, N.; Apostol, V. Drought Conditions and Management Strategies in Romania (Capacity Development to Support National Drought Management Policy) [Country Report]. Available online: https://www.droughtmanagement.info/literature/UNW-DPC_NDMP_Country_Report_Romania_2013.pdf (accessed on 11 July 2015).
76. Prăvălie, R.; Sirodoev, I.; Patriche, C.V.; Bandoc, G.; Peptenatu, D. The analysis of the relationship between climatic water deficit and corn agricultural productivity in the Dobrogea plateau. *Carpathian J. Earth Environ. Sci.* **2014**, *9*, 201–214.
77. Prăvălie, R.; Bandoc, G. Aridity Variability in the Last Five Decades in the Dobrogea Region, Romania. *J. Arid. Land Res. Manag.* **2015**, *29*, 265–287. [CrossRef]
78. Dumitru, A.; Olaru, E.-A.; Dumitru, M.; Iorga, G. Assessment of air pollution by aerosols over a coal open-mine influenced region in southwestern Romania. *Rom. J. Phys.* **2024**, *69*, 801. [CrossRef]
79. Chiritescu, R.-V.; Luca, E.; Iorga, G. Observational study of major air pollutants over urban Romania in 2020 in comparison with 2019. *Rom. Rep. Phys.* **2024**, *76*, 702.
80. Serban, C.; Maftei, C. Spatiotemporal Drought Analysis Using the Composite Drought Index (CDI) over Dobrogea, Romania. *Water* **2025**, *17*, 481. [CrossRef]
81. Popescu, A.; Dinu, T.A.; Stoian, E.; Serban, V. Variation of the main agricultural crops yield due to drought in Romania and Dobrogea region in the period 2000–2019. *Sci. Pap. Ser. Manag. Econ. Eng. Agric. Rural. Dev.* **2020**, *20*, 397–415.
82. Ranca, A. Climate Changes and Their Impact on the Vineyards in Dobrogea. Available online: https://climatechange-summit.org/climate-change-and-its-influence-on-romanian-wine-the-case-of-dobrogea/#:~:text=Climate%20change%20and%20its%20influence%20on%20Romanian%20wine%20%E2%80%93%20the%20case,and%20quality%20of%20native%20wines (accessed on 11 July 2024).
83. Gâştescu, P. The Danube Delta Biosphere Reserve. Geography, Biodiversity, Protection, Management. Available online: https://www.limnology.ro/water2012/Proceedings/066.pdf (accessed on 4 June 2025).
84. ClimateChangePost. Droughts. Romania. Available online: https://www.climatechangepost.com/countries/romania/droughts/ (accessed on 16 July 2025).
85. Bărbulescu, A.; Serban, C.; Maftei, C. Statistical analysis and evaluation of Hurst coefficient for annual and monthly precipitation time series. *WSEAS Trans. Math.* **2010**, *9*, 791–800.

86. Lelieveld, J.; Hadjinicolaou, P.; Kostopoulou, E.; Chenoweth, J.; El Maayar, M.; Giannakopoulos, C.; Hannides, C.; Lange, M.A.; Tanarhte, M.; Tyrlis, E.; et al. Climate change and impacts in the Eastern Mediterranean and the Middle East. *Clim. Change* **2012**, *114*, 667–687. [CrossRef] [PubMed]
87. Prăvălie, R.; Piticar, A.; Roșca, B.; Sfîcă, L.; Bandoc, G.; Tiscovschi, A.; Patriche, C. Spatio-temporal changes of the climatic water balance in Romania as a response to precipitation and reference evapotranspiration trends during 1961–2013. *Catena* **2019**, *172*, 295–312. [CrossRef]
88. Cheval, S.; Dumitrescu, A.; Birsan, M.-V. Variability of the aridity in the South-Eastern Europe over 1961–2050. *Catena* **2017**, *151*, 74–86. [CrossRef]
89. Bărbulescu, A. On the Regional Temperature Series Evolution in the South-Eastern Part of Romania. *Appl. Sci.* **2023**, *13*, 3904. [CrossRef]
90. Tolika, K.; Anagnostopoulou, C.; Traboulsi, M.; Zaharia, L.; (Oprea) Constantin, D.M.; Tegoulias, I.; Maheras, P. Comparative Study of the Frequencies of Atmospheric Circulation Types at Different Geopotential Levels and Their Relationship with Precipitation in Southern Romania. Available online: https://www.thefreelibrary.com/Comparative%2BStudy%2Bof%2Bthe%2BFrequencies%2Bof%2BAtmospheric%2BCirculation%2BTypes...-a0811216020?utm_source=chatgpt.com (accessed on 10 June 2025).
91. Pascale, S.; Lucarini, V.; Feng, X.; Porporato, A.; ul Hasson, S. Projected Changes of Rainfall Seasonality and Dry Spells in a High Concentration Pathway 21st Century Scenario. *arXiv* **2014**, arXiv:1410.3116. [CrossRef]
92. Bădăluță, C.A.; Haliuc, A.; Bădăluță, G.; Scriban, R.E. Spatiotemporal variability of drought in Romania during 1901–2021 using the Standardized Precipitation Evapotranspiration Index (SPEI). *An. Univ. Oradea Ser. Geogr.* **2024**, *34*, 33–44. [CrossRef]
93. Bandoc, G.; Prăvălie, R. Climatic water balance dynamics over the last five decades in Romania's most arid region, Dobrogea. *J. Geogr. Sci.* **2015**, *25*, 1307–1327. [CrossRef]
94. European Environment Agency. Coastal. Available online: https://www.eea.europa.eu/publications/europes-changing-climate-hazards-1/coastal (accessed on 16 July 2025).
95. Climate ADAPT. Coastal Areas. Available online: https://climate-adapt.eea.europa.eu/en/eu-adaptation-policy/sector-policies/coastal-areas#:~:text=Climate%20change%20is%20expected%20to,coastal%20areas%20at%20EU%20levels (accessed on 16 July 2025).
96. Climate Risk in the Agricultural Sector. Available online: https://www.unepfi.org/wordpress/wp-content/uploads/2023/03/Agriculture-Sector-Risks-Briefing.pdf (accessed on 16 July 2025).
97. Bărbulescu, A.; Maftei, C.; Dumitriu, C.S. The modelling of the climateric process that participates at the sizing of an irrigation system. *Bull. Appl. Comput. Math.* **2002**, *2048*, 11–20.
98. *State of Food and Agriculture*; Food and Agriculture Organization of the United Nations: Rome, Italy, 2020. Available online: https://openknowledge.fao.org/server/api/core/bitstreams/6e2d2772-5976-4671-9e2a-0b2ad87cb646/content#:~:text=drink%20and%20water%20to%20grow,alia%2C%20supporting%20inland%20fisheries%20and (accessed on 16 July 2025).
99. Romania—2016–2020 National Action Plan on Climate Change: Summary Report (English). Dissemination Note. World Bank Group: Washington, DC, USA. Available online: https://documents1.worldbank.org/curated/en/254931468188327164/pdf/103920-WP-P145943-PUBLIC-Summary-of-Climate-Change-Action-Plan.pdf (accessed on 16 July 2025).
100. Rus, M.-I.; Munteanu, I.; Vaidianu, N.; Aivaz, K.-A. Research Trends Concerning the Danube Delta: A Specific Social-Ecological System Facing Climate Uncertainty. *Earth* **2025**, *6*, 7. [CrossRef]
101. Better Water Quality Using Integrative Floodplain Management Based on Ecosystems Services. Available online: https://dtp.interreg-danube.eu/uploads/media/approved_project_output/0001/56/be4e1449db0a518c6391634bbca0dc083dbe8533.pdf (accessed on 16 July 2025).